TẠP CHÍ KHOA HỌC & CÔNG NGHỆ ĐẠI HỌC DUY TÂN
DTU Journal of Science and Technology 5(54) (2022) 27-36

TRƯỜNG ĐẠI HỌC DUY TÂN
DUYTAN UNIVERSITY

Influence of rice husk ash on mortar compressive strength at different temperatures: Machine learning based modelling

Ảnh hưởng của tro trấu tới cường độ của vữa ở các nhiệt độ khác nhau: Mô hình hóa bằng máy học

Tran Thu Hien[a,b*], Hoang Nhat Duc[a,b]
Trần Thu Hiền[a,b*], Hoàng Nhật Đức[a,b]

[a]*Institute of Research and Development, Duy Tan University, Da Nang, 550000, Vietnam*
[a]*Viện Nghiên cứu và Phát triển Công nghệ Cao, Đại học Duy Tân, Đà Nẵng, Việt Nam*
[b]*Faculty of Civil Engineering, Duy Tan University, Da Nang, 550000, Vietnam*
[b]*Khoa Xây dựng, Trường Đại học Duy Tân, Đà Nẵng, Việt Nam*

(Ngày nhận bài: 07/3/2022, ngày phản biện xong: 24/5/2022, ngày chấp nhận đăng: 30/8/2022)

Abstract

The impact of different rice husk ash contents (5, 10, 20%) on mortar strength is examined at different elevated temperatures (150, 300, 450, 750°C). Based on a 45 experimental result data set, three machine learning algorithms including the Artificial Neural Network (ANN), the Least Squares Support Vector Regression (LS-SVR) and the Multivariate Adaptive Regression Splines (MARS) have been used to model the functional relationship between the mixture components and the compressive strength. As a result, it is shown that LS-SVR consists in the most capable approach for modeling mortar strength with a good value of coefficient of determination (R^2) = 0.80. Accordingly, this machine learning approach is potential to be used in RHA contained mix design by construction engineers.

Keywords: Compressive Strength; Elevated Temperature; Rice Husk Ash; Mortar; Machine Learning.

Tóm tắt

Ảnh hưởng của hàm lượng tro trấu (5, 10, 20%) tới cường độ của vữa được nghiên cứu tại các nhiệt độ khác nhau gồm 150, 300, 450, 750°C. Dựa trên 45 kết quả thí nghiệm, ba thuật toán máy học gồm Mạng thần kinh nhân tạo, Vec tơ hồi quy bình phương tối thiểu (LS-SVR), và Hồi quy thích ứng đa biến (MARS) được sử dụng để mô hình hóa mối quan hệ giữa các thành phần và cường độ vữa. Kết quả thu được cho thấy phương pháp Vectơ hồi quy bình phương tối thiểu mô hình chính xác nhất với hệ số R^2 = 0.80. Như vậy, mô hình hóa bằng máy học hoàn toàn có thể được sử dụng để thiết kế hỗn hợp vữa chứa RHA theo cường độ.

Từ khóa: Cường độ chịu nén; Nhiệt độ cao; Tro trấu; Vữa; Máy học.

1. Introduction

Concrete is recognized as one of the most widely used construction material. It is estimated that the average consumption of concrete is about 1 ton per year per every person on the planet [1]. However, the production of cement and concrete are associated with a significant environmental issue. Indeed, cement consists in concrete's ingredient that contributes most to its embodied

[*]*Corresponding Author:* Tran Thu Hien, Institute of Research and Development, Duy Tan University, Da Nang, 550000, Vietnam; Faculty of Civil Engineering, Duy Tan University, Da Nang, 550000, Vietnam
Email: tranthuhien4@dtu.edu.vn

energy. To produce 1 ton of cement in the optimal conditions, about 3 GJ of energy must be provided. In addition, cement is the largest source emission of CO_2, followed by aggregate, accounting for 74-81% and 13-20% of the total amount CO_2 yielded from the production of concrete [1]. Every kilogram of cement produced will release about 0.7-1.0 kg of CO_2 gas. The CO_2 emission result from the calcite decomposition, the fuel combustion, and the transportation of cement between production and consumption sites, etc. Generally, the CO_2 amount released by the cement industry accounts for 5-7% of global emissions from all sectors [2].

Several solutions have been conducted to reduce the environmental impact of cement production, such as the change in the chemical composition of clinker, the use of alternative fuels, and other alternatives. One of the most promising solution is to minimize the clinker amount by maximizing the supplementary cementitious materials used in cement and promoting the use of blended cement [3].

Among the mineral admixtures produced annually, such as fly ash (500 million tons), limestone (170 million tons), blast-furnace slag (75 million tons), rice husk ash with an output of about 37 million tons represents a promising replacing cementitious material [4]. The research on mortar or concrete mixtures incorporating RHA has attracted the attention of various scholars. Rukzon and Chindaprasirt [5] studied the strength and carbonation resistance of mortar mixture that employs portland rice husk ash cement. As a result, this works demonstrated that the inclusion of rice husk ash produces mortar mixtures with good strength and low porosity. Antiohos et al. [6] examined the pozzolanic properties of untreated RHA and its impact on the mortar strength, capillarity absorption, permeability and diffusion.

Islam, et al. [7] established a statistical model for predicting the strength and slump of RHA incorporated high-performance concrete; the model constructed by regression analysis technique was able to yield well estimated properties of concrete containing RHA. Ambas, et al. [8] also constructed regression equations from experimental data to predict the compressive strength of a cement mortar with RHA replacement. Genetic programming approach have been employed by Sarıdemir [9] for predicting compressive strength of concretes containing rice husk ash; this research showed the strong potentiality of this learning method in the task of interest.

This research is dedicated to the extension of the body of knowledge by proposing the application of three machine learning models for predicting compressive strength of mortar mixtures containing RHA. The Artificial Neural Network (ANN), Least Squares Support Vector Regression (LS-SVR) and Multivariate Adaptive Regression Splines (MARS) models were selected.

2. Research method

2.1. Description of experiments with mortar

In order to investigate the effect of RHA on the compressive strength of the samples (Y), this study has collected 45 testing results. The six variables including RHA replacement percentage (X_1), cement (X_2), RHA (X_3), superplasticizer (X_4), heating temperature (X_5), and mortar age (X_6) are employed as influencing factors to estimate the sample compressive strength. The scatter plots of variables and the detailed description of several statistical properties of the variables are provided in **Fig. 1** and **Table 1**, respectively.

Table 1. Mortar compositions

Variables	Unit	Min	Average	Std.	Max
Rice husk ash replacement percentage	%	0.00	13.00	11.00	30.00
Cement	g	315.00	391.50	48.47	450.00
Rice husk ash	g	0.00	58.50	48.47	135.00
Superplasticizer	mL	0.00	0.77	0.89	2.40
Heating Temperature	^{o}C	27.00	198.33	242.01	750.00
Age	day	3.00	37.67	21.59	56.00
Compressive strength	MPa	0.00	42.99	22.24	75.02

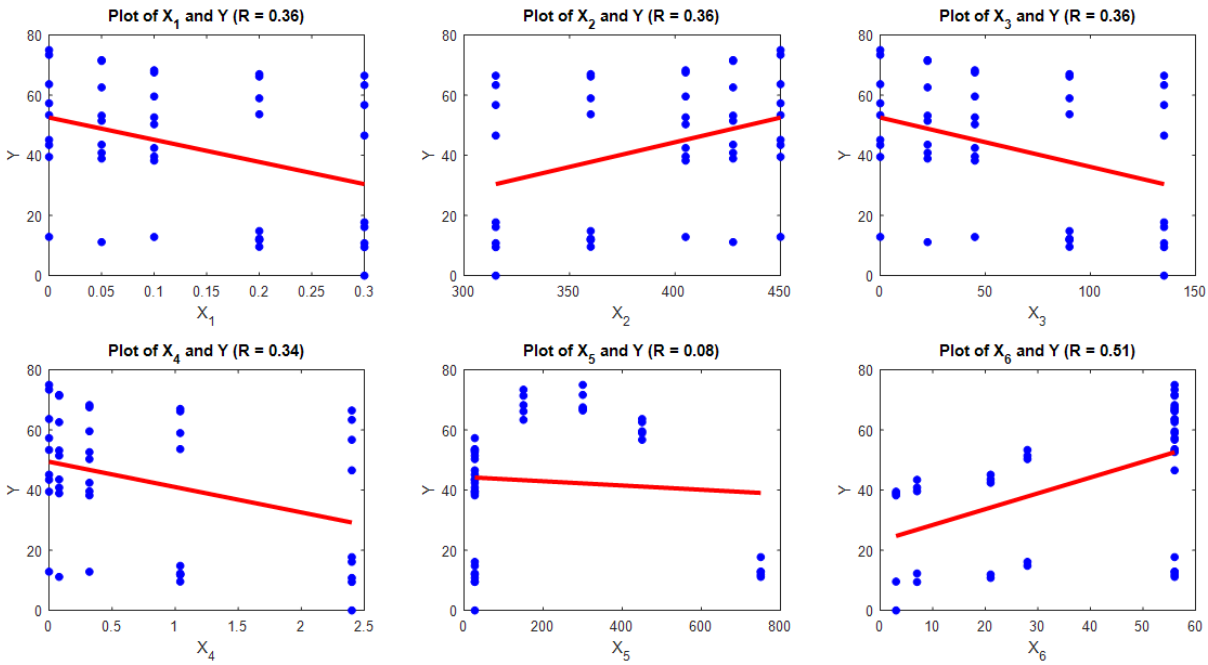

Fig. 1 Scatter plots of influencing factors

2.2. Machine learning methods

2.2.1. Artificial Neural Network (ANN)

ANN consists in a machine learning approach based on the biological neural networks which allows simulating the learning and inference processes of the human brain [10]. The advantages of the ANN consist in universal learning capability, fast computation, and good performance in nonlinear modeling [11]. Since ANN is a supervised learning approach, the learning task is to construct a function $f : X \in R^D \rightarrow Y \in R^1$ from the collected data, where D denotes the number of attributing input. A typical ANN model consisting of the input, hidden, and output layers, is illustrated in **Fig. 2**. W_1 and W_2 denote the weight matrices of the hidden layer and the output layer, respectively; N represents the number of neurons in the hidden layer; b_1 = [b_{11}, $b_{12,}$…, b_{1N}] and b_2 are a bias vector of the hidden layer and of the output layer, respectively; f_A represents an activation function. The commonly employed activation function is the log-sigmoid.

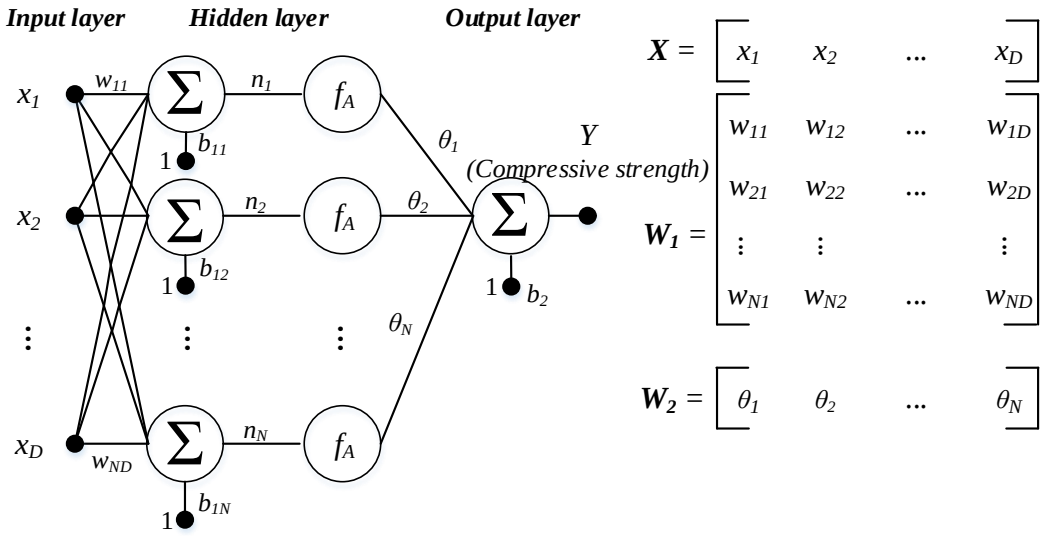

Fig. 2 A typical Artificial Neural Network structure

The overall structure of ANN model for regression analysis is given as follows [12]:

$$f(X) = b_2 + W_2 \times (f_A(b_1 + W_1 \times X)) \quad (1)$$

The model structure of an ANN including the weight matrices and the bias are adapted through a process of error backpropagation [13]. Moreover, the Mean Square Error (MSE) is employed as the objective function for training an ANN structure for regression analysis problems [14]:

$$MSE = \min_{W_1, W_2, b_1, b_2} \frac{1}{M} \sum_{i=1}^{M} e_i^2 \quad (2)$$

where M denotes the number of data samples; e_i represents an output error. $e_i = Y_{i,P} - Y_{i,A}$ ($Y_{i,P}$ and $Y_{i,A}$ are the predicted and actual outputs, respectively).

2.2.2. Multivariate Adaptive Regression Splines

MARS [15] is a non-parametric regression method for constructing modeling equations directly from the collected data. This approach divides the original learning space into several sub-ranges of the prediction variables in order to establish a functional relationship between the influencing variables and the predicted variable [16]. MARS relies on a piecewise linear function for characterizing each local model and uses an adaptive mechanism to establish the final prediction model [17]. Previous research works [18-20] have approved the predictive capability of MARS in resolving various complex problems in the engineering field. The prediction model constructed by MARS is constructed through a set of basis functions (*BF*s) which describes the relationship between influencing factors and modeled output. A typical form of a *BF* is given as follows:

$$b_m(x) = \max(0, C - x) \ \ or \quad b_m(x) = \max(0, x - C) \quad (3)$$

where b_m is a *BF*; x denotes an input variable; C is a threshold parameter used to divide the original range of x into sub-ranges.

The final functional form of the MARS prediction model is given as follows:

$$f(x) = \alpha_0 + \sum_{m=1}^{k} \alpha_m b_m(x) \quad (4)$$

where $\alpha_0, \alpha_1, ..., \alpha_M$ denote weighting coefficients; $f(x)$ is the model output. k represents the number of weighting coefficients.

It is noted that the model construction of MARS is divided into two phases: forward and

backward phases (see **Fig. 3**). In the first phase, *BF*s are added into the model to minimize the training error; this phase will be stopped when the maximum number of *BF* is reached. The second phase is to fend off overfitting problem by casting out several redundant *BF*s. In other words, the second phase aims at simplifying the model structure.

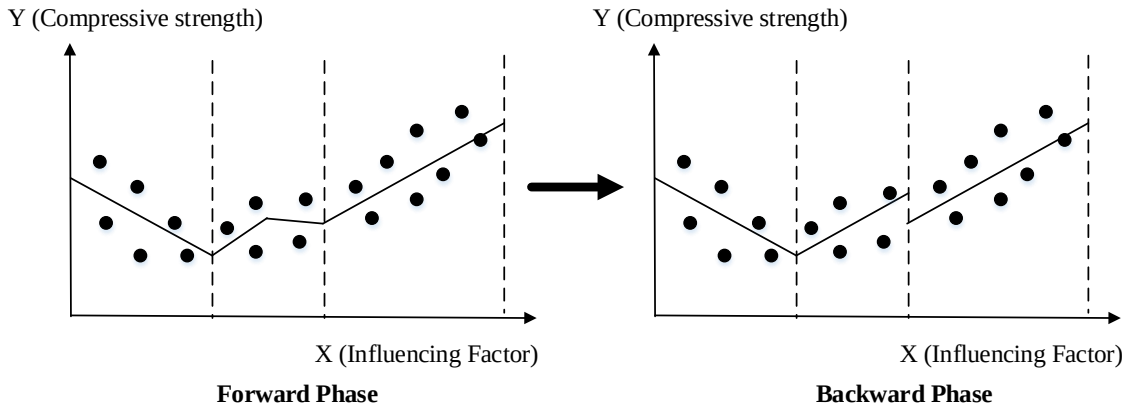

Fig. 3 Illustration of the MARS model learning phases

Moreover, each sub-model of MARS is assessed by the generalized cross-validation (GCV) index [21, 22] as shown as follows:

$$\mathrm{GCV} = \mathrm{MSE} / (1 - \frac{k + 0.5c(k-1)}{n})^2 \quad (5)$$

where MSE denotes the mean square error of the model, *k* is the number of *BF*s. *n* denotes the number of observations in the training data. *c* represents a penalty coefficient; Friedman [15] and Jekabsons [22] suggested that the appropriate value of the parameter *c* should be in the range of [2, 4].

2.2.3. Least Squares Support Vector Regression (LS-SVR)

Proposed by Suykens et al. [23], LS-SVR is a computational intelligence approach which relies on the principal of structural risk minimization. This approach has been proved to be very effective in modeling complex engineering processes [24]. Compared to the standard Support Vector Machine, the learning phase of LS-SVR can be accomplished with less computational expense, because the training LS-SVR process only needs solving a set of linear equations [23, 25].

To construct a regression model, it is required to prepare a dataset of mortar test samples in the following form: $D = \{x_k, y_k\}$, $k = 1,2,...,N$. It is noted that *k* is the *k*th data sample and *N* represents the total number of data samples. It is noted that x_k is a vector with input variables. In addition, y_k represents the output of mortar compressive strength of the *k*th testing sample. LS-SVR constructs a functional mapping $y(x)$ that computes the mortar compressive strength based on the input vector *x* that provides the information of mix components. Because the mapping function $y(x)$ is possibly nonlinear, LS-SVR first transforms the input data from the original input space of six dimensions to a high dimensional feature space. This transformation is achieved through a mapping function $\phi(x)$. Hence, the original nonlinear regression problem is converted to a linear one in the new learning space. The learning concept of LS-SVR is illustrated in **Fig. 4**.

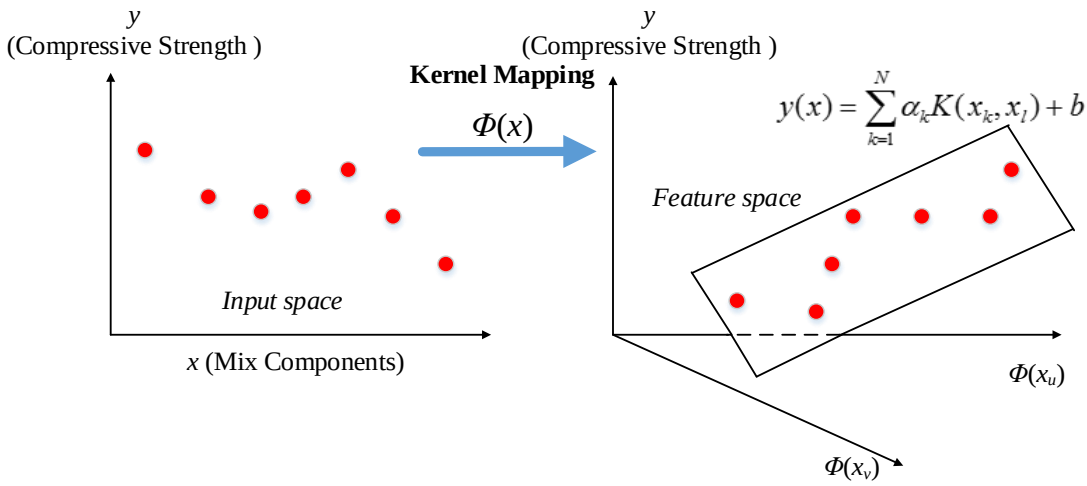

Fig. 4 LS-SVR for concrete compressive strength modeling

In the training phase, the model structure of LS-SVR is learnt by solving the following optimization problem [23]:

$$\text{Minimize } J_p(w,e)=\frac{1}{2}w^T w+\gamma\frac{1}{2}\sum_{k=1}^{N}e_k^2 \quad (6)$$

$$\text{Subjected to } y_k=w^T\phi(x_k)+b+e_k,\ k=1,...,N$$

where $e_k\in R$ denotes error variables; $\gamma>0$ is a regularization constant.

To solve the aforementioned optimization problem, the Lagrangian is constructed as follows [23]:

$$L(w,b,e;\alpha)=J_p(w,e)-\sum_{k=1}^{N}\alpha_k\{w^T\phi(x_k)+b+e_k-y_k\} \quad (7)$$

where α_k is a Lagrange multiplier.

The Karush–Kuhn–Tucker conditions for optimality are employed by differentiating the Lagrangian function L(w,b,e,α) with the input variables in the following manner [23]:

$$\begin{cases}\dfrac{\partial L}{\partial w}=0\rightarrow w=\sum_{k=1}^{N}\alpha_k\phi(x_k)\\ \dfrac{\partial L}{\partial b}=0\rightarrow\sum_{k=1}^{N}\alpha_k=0\\ \dfrac{\partial L}{\partial e_k}=0\rightarrow\alpha_k=\gamma e_k,\ k=1,...,N\\ \dfrac{\partial L}{\partial \alpha_k}=0\rightarrow w^T\phi(x_k)+b+e_k-y_k=0,\ k=1,...N\end{cases} \quad (8)$$

After solving the above linear system, the final LS-SVR model is shown as follows [23, 26]:

$$y(x_l)=\sum_{k=1}^{N}\alpha_k K(x_k,x_l)+b \quad (9)$$

where α_k and b denote the solution to the linear system. k and N denote the index and the total number of data samples. x_k and x_l are two input samples in the training and testing set, respectively.

Moreover, $K(.)$ represents the kernel function which maps the input data from the feature space into the high-dimensional space. The radial basis kernel function is often selected to be used in LS-SVR [27]; this function is given as follows [23, 28]:

$$K(x_k,x_l)=\exp\left(-\frac{\|x_k-x_l\|^2}{2\sigma^2}\right) \quad (10)$$

where σ represents the radial basis kernel function parameter.

3. Experimental result and comparison

Because the problem of interest is formulated as a supervised learning, the data set, which includes 45 experimental tests, is randomly divided into the training set (90%) and the testing set (10%). These two sets are employed to construct and to verify the three employed machine learning models. In

addition, to reliably assess the performance of these prediction models, the training and testing phases are carried out 20 times via a random subsampling process. In addition, the Root Mean Squared Error (RMSE) and the coefficient of determination (R^2) are employed to quantify the prediction accuracy of the machine learning models. The RMSE exhibits the deviation between the compressive strength values actually observed and the compressive strength values predicted from a model. Meanwhile, the R^2 quantifies the proportion of the variability in the compressive strength explained by the model; R^2 indicates how well a machine learning model regresses the output value of interest on the input variables of mortar components.

It is noted that the implementation of the ANN model relies on the MATLAB toolbox of Statistics and Machine Learning [29]. The training and prediction phases of LS-SVR is operated via the toolbox developed by De Brabanter, et al. [30]. In addition, the implementation of MARS is based on the toolbox provided by Jekabsons [22]. Prior to the model construction phases of ANN, LS-SVR, and MARS, it is necessary to determine appropriate tuning parameters of those models. This task is widely known as mode selection. In this study, a five-fold cross-validation process [31] is employed to identify desired values of the models' tuning parameters. The most suitable set of tuning parameters of each model is associated with the model with the minimal value of the average RMSE in the testing phase.

To identify an appropriate configuration of the ANN model, it is required to set the number of neurons, the learning rate, the activation function, and the number of training epochs. The activation function and the number of training epochs are not very sensitive to the prediction outcome of ANN. In this study, the log-sigmoid function is selected as the activation function and the number of training epochs is fixed to be 5000. A five-fold cross-validation process [31] is employed to identify desired values of the number of neurons in the hidden layer and the learning rate. The experimental results revealed that the number of neurons = 6 and the learning rate = 0.01 are a good setting of tuning parameters. Furthermore, MARS requires choosing the specification of the maximum number of basis functions (k_{max}) and the penalty coefficient (c). The appropriate values of MARS are as follows: k_{max} = 15 and c = 2.5. For the case of LS-SVR, the values of the regularization parameter (γ) and the kernel function parameter (σ) are found to be 100 and 5, respectively.

Table 2. Result Comparison

Phase	Performance	ANN		LS-SVR		MARS	
		Mean	Std	Mean	Std	Mean	Std
Training	RMSE	5.40	3.17	5.73	0.11	4.35	0.90
	R^2	0.92	0.10	0.93	0.00	0.96	0.01
Testing	RMSE	**8.20**	**5.78**	**7.28**	**2.51**	**7.86**	**3.49**
	R^2	**0.70**	**0.53**	**0.80**	**0.26**	**0.74**	**0.26**

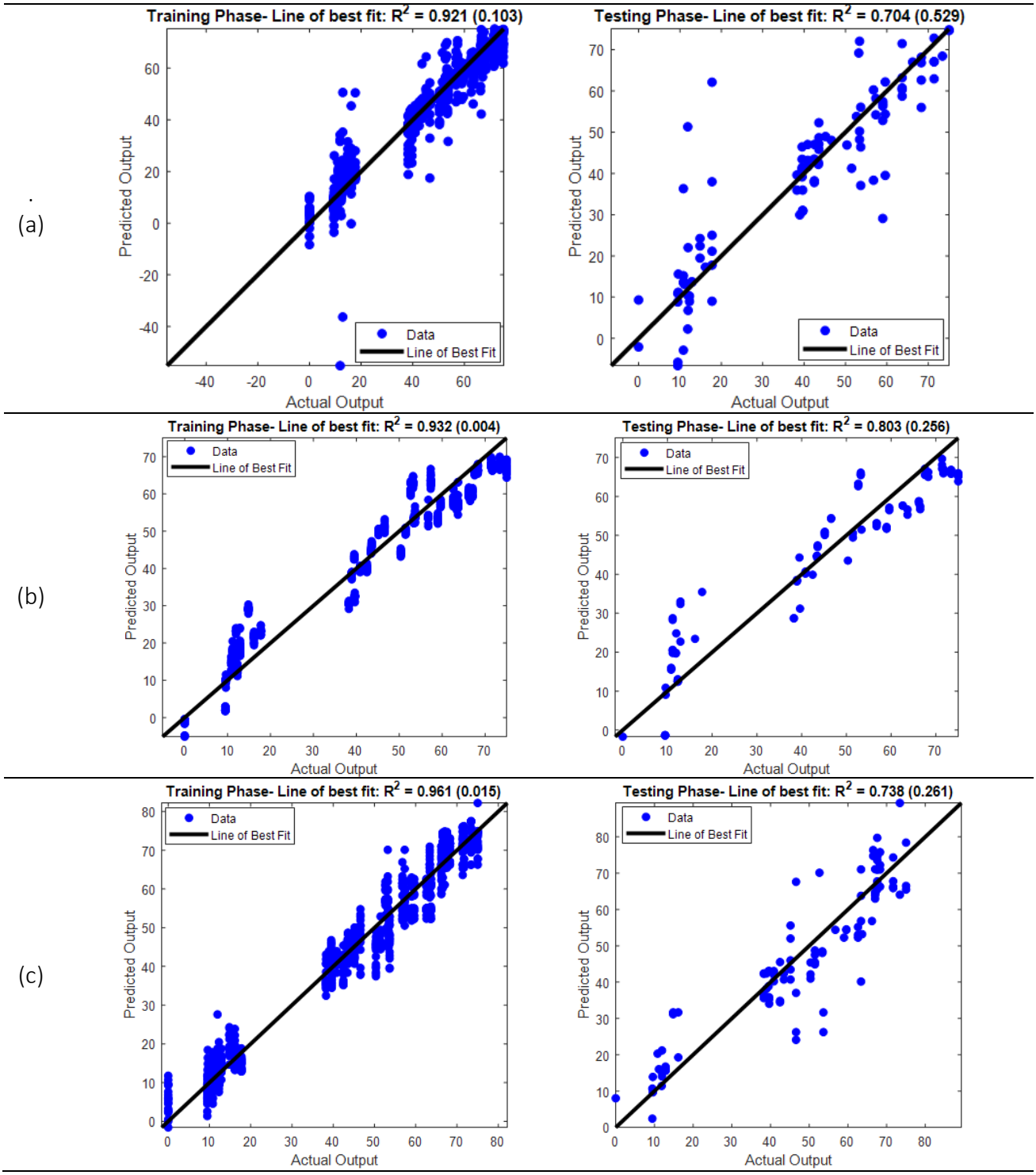

Fig. 5 Model Prediction Results: (a) ANN, (b) LS-SVR, and (c) MARS

Detail of the prediction result of all the models obtained from the repeated subsampling process is reported in **Table 2**. As aforementioned, RMSE and R^2 of each model in both training and testing phases are presented to quantify the model predictive capability. In addition, the average value (mean) and standard deviation (Std) of the results are computed. It is observable that LS-SVR has achieved the best prediction performance in the testing phase with RMSE = 7.28 and R^2 = 0.80, followed by MARS (RMSE = 7.86 and R^2 = 0.74) and ANN (RMSE = 8.20 and R^2 = 0.70). Thus, the prediction performance of LS-SVR is found to

be superior to those of MARS and ANN. The details of the prediction outcomes of the three models are graphically described in **Fig. 5.**

4. Conclusion

Motivated by the economic and environmental benefits of using RHA as a cement replacement material, this paper has investigated the durability, reflected by compressive strength, of mortar mixes containing RHA. Based on the collected data set, three machine learning algorithms, including ANN, LS-SVR, and MARS, have been employed to learn the functional mapping between mixture component and the sample strength. Based on a repeated sub-sampling procedure, LS-SVR has been identified as the most appropriate approach for modeling the collected data set with a good value of R^2 = 0.80. Hence, the prediction model constructed by LS-SVR can be useful for assisting construction engineers in mixture design tasks. The future direction of the current study includes the extension of the current data set to enhance its variability as well as the investigation of other advanced machine learning methods to improve the modeling accuracy of the compressive strength of the RHA contained mortar mixes.

References

[1] D. Flower and J. Sanjayan (2007), *Green house gas emissions due to concrete manufacture*, *Int J LCA*, vol. 12, pp. 282-288.

[2] K. Humphreys and M. Mahasenan (2002), *Toward a sustainable cement industry, Substudy 8, climate change*. World Business council for sustainable development.

[3] P. K. Mehta. (2009), *Global concrete industry sustainability*, Concrete International, vol. 31, pp. 45-48.

[4] V. T. Nguyen, Y. Guang, V. B. Klaas, A. L. A. Fraaj, and D. D. Bui (2011), *The study of using rice husk ash to produce ultra high performance concrete*, Construction and Building Materials, vol. 25, pp. 2030-35.

[5] S. Rukzon and P. Chindaprasirt (2010), *Strength and Carbonation Model of Rice Husk Ash Cement Mortar with Different Fineness*, Journal of Materials in Civil Engineering, vol. 22, pp. 253-259

[6] S. K. Antiohos, J. G. Tapali, M. Zervaki, J. Sousa-Coutinho, S. Tsimas, and V. G. Papadakis. (2013), *Low embodied energy cement containing untreated RHA: A strength development and durability study*, Construction and Building Materials, vol. 49, pp. 455-463.

[7] M. N. Islam, M. F. Mohd Zain, and M. Jamil (2012), "Prediction of Strength and Slump of Rice Husk Ash Incorporated High-Performance Concrete," *Journal of Civil Engineering and Management*, vol. 18, pp. 310-317.

[8] D. T. Ambas, G. M. C. D. Rosa, L. J. A. Esquejo, J. D. Gil, M. L. Magtalas, C. J. D. Rubinas, et al (2015), *Effect of Rice Husk Ash as cement replacement in the compressive strength of hydraulic cement mortar cube*, in International Conference on Humanoid, Nanotechnology, Information Technology,Communication and Control, Environment and Management (HNICEM), 2015, pp. 1-3.

[9] M. Sarıdemir (2010), *Genetic programming approach for prediction of compressive strength of concretes containing rice husk ash*, Construction and Building Materials, vol. 24, pp. 1911-1919.

[10] C. Bishop (1995), *Neural Networks For Pattern Recognition*, Clarendon Press, Oxford, 1995.

[11] T.-H. Tran and N.-D. Hoang (2016), *Predicting Colonization Growth of Algae on Mortar Surface with Artificial Neural Network*, Journal of Computing in Civil Engineering, vol. 30, pp. 04016030.

[12] M. H. Beale, M. T. Hagan, and H. B. Demuth (2012), *Neural Network Toolbox User's Guide*, The MathWorks, Inc, 2012.

[13] N.-D. Hoang and D. Tien Bui (2017), *GIS-Based Landslide Spatial Modeling Using Batch-Training Back-propagation Artificial Neural Network: A Study of Model Parameters*, in Advances and Applications in Geospatial Technology and Earth Resources: Proceedings of the International Conference on Geo-Spatial Technologies and Earth Resources 2017

[14] B. T. Pham, D. Tien Bui, I. Prakash, and M. B. Dholakia (2017), *Hybrid integration of Multilayer Perceptron Neural Networks and machine learning ensembles for landslide susceptibility assessment at Himalayan area (India) using GIS*, CATENA, vol. 149, Part 1, pp. 52-63.

[15] J. H. Friedman (1991), *Multivariate Adaptive Regression Splines, Ann. Statist*., vol. 19, pp. 1-67.

[16] A. Parsaie, A. H. Haghiabi, M. Saneie, and H. Torabi (2016), *Prediction of energy dissipation on the stepped spillway using the multivariate adaptive regression splines*, ISH J. Hydraul. Eng., vol. 22, pp. 281-292.

[17] N.-D. Hoang, C.-T. Chen, and K.-W. Liao (2017), *Prediction of chloride diffusion in cement mortar using Multi-Gene Genetic Programming and Multivariate Adaptive Regression Splines*, Measurement, vol. 112, pp. 141-149.

[18] A. T. C. Goh, Y. Zhang, R. Zhang, W. Zhang, and Y. Xiao (2017), E*valuating stability of underground entry-type excavations using multivariate adaptive regression splines and logistic regression*, Tunnelling and Underground Space Technology, vol. 70, pp. 148-154.

[19] A. Ferreira-Santiago, C. López-Martín, and C. Yáñez-Márquez (2016), *Metaheuristic optimization of multivariate adaptive regression splines for predicting the schedule of software projects*, Neural Comput. Appl., vol. 27, pp. 2229-2240.

[20] M.-Y. Cheng and M.-T. Cao (2016), *Estimating strength of rubberized concrete using evolutionary multivariate adaptive regression splines*, J. Civ. Eng. Manag., vol. 22, pp. 711-720.

[21] S. Suman, S. K. Das, and R. Mohanty (2016), *Prediction of friction capacity of driven piles in clay using artificial intelligence techniques*, International Journal of Geotechnical Engineering, vol. 10, pp. 469-475.

[22] G. Jekabsons (2016), *ARESLab: Adaptive Regression Splines toolbox for Matlab/Octave*, Technical report, Riga Technical University, available at http://www.cs.rtu.lv/jekabsons/.

[23] J. Suykens, J. V. Gestel, J. D. Brabanter, B. D. Moor, and J. Vandewalle (2002), *Least Square Support Vector Machines*, World Scientific Publishing Co. Pte. Ltd., Singapore.

[24] S. Xu, Z. Liu, and Y. Zhang (2015), *Least squares support vector regression and interval type-2 fuzzy density weight for scene denoising*, Soft Computing, pp. 1-12.

[25] T.-H. Tran and N.-D. Hoang (2017), *Estimation of algal colonization growth on mortar surface using a hybridization of machine learning and metaheuristic optimization*, Sādhanā, vol. 42, pp. 929-939.

[26] J. Ji, C. Zhang, Y. Gui, Q. Lü, and J. Kodikara (2016), *New Observations on the Application of LS-SVM in Slope System Reliability Analysis*, J. Comput. Civ. Eng., vol. Just Released, p. 06016002.

[27] D. Tien Bui, K.-T. T. Bui, Q.-T. Bui, C. V. Doan, and N.-D. Hoang (2017), *Chapter 15 - Hybrid Intelligent Model Based on Least Squares Support Vector Regression and Artificial Bee Colony Optimization for Time-Series Modeling and Forecasting Horizontal Displacement of Hydropower Dam*, in Handbook of Neural Computation, ed: Academic Press, pp. 279-293.

[28] D. Yao, J. Yang, X. Li, and C. Zhao (2016), *A Hybrid Approach for Fault Diagnosis of Railway Rolling Bearings Using STWD-EMD-GA-LSSVM*, Mathematical Problems in Engineering, vol. 2016, p.7.

[29] Mathworks (2016), *Statistics and Machine Learning Toolbox*, The MathWorks, Inc..

[30] K. De Brabanter, P. Karsmakers, F. Ojeda, C. Alzate, J. De Brabanter, K. Pelckmans, et al. (2010), *LS-SVMlab Toolbox User's Guide version 1.8*, Internal Report 10-146, ESAT-SISTA, K.U.Leuven (Leuven, Belgium).

[31] M.-Y. Cheng and N.-D. Hoang (2014), *Groutability prediction of microfine cement based soil improvement using evolutionary LS-SVM inference model*, J. Civ. Eng. Manag., vol. 20, pp. 1-10.